doi:10.1093/brain/awz070 BRAIN 2019: 142; 1349–1364 | 1349

BRAIN
A JOURNAL OF NEUROLOGY

Reactivation of nonsense-mediated mRNA decay protects against *C9orf72* dipeptide-repeat neurotoxicity

Wangchao Xu,[1,2] Puhua Bao,[1] Xin Jiang,[1,2] Haifang Wang,[1] Meiling Qin,[1] Ruiqi Wang,[1] Tao Wang,[1] Yi Yang,[1,2] Ileana Lorenzini,[3] Lujian Liao,[4] Rita Sattler[3] and Jin Xu[1]

Amyotrophic lateral sclerosis is a deleterious neurodegenerative disease without effective treatment options. Recent studies have indicated the involvement of the dysregulation of RNA metabolism in the pathogenesis of amyotrophic lateral sclerosis. Among the various RNA regulatory machineries, nonsense-mediated mRNA decay (NMD) is a stress responsive cellular surveillance system that degrades selected mRNA substrates to prevent the translation of defective or harmful proteins. Whether this pathway is affected in neurodegenerative diseases is unclear. Here we report the inhibition of NMD by arginine-rich dipeptide repeats derived from *C9orf72* hexanucleotide repeat expansion, the most common cause of familial amyotrophic lateral sclerosis. Bioinformatic analysis of multiple transcriptome profiles revealed significant overlap of upregulated genes in NMD-defective cells with those in the brain tissues, micro-dissected motor neurons, or induced pluripotent stem cell-derived motor neurons specifically from amyotrophic lateral sclerosis patients carrying *C9orf72* hexanucleotide repeat expansion, suggesting the suppression of NMD pathway in these patients. Using *Drosophila* as a model, we have validated that the *C9orf72* hexanucleotide repeat expansion products could lead to the accumulation of the NMD substrates and identified arginine-rich dipeptide repeats, including poly glycine-arginine and poly proline-arginine, as the main culprits of NMD inhibition. Furthermore, in human SH-SY5Y neuroblastoma cells and in mouse brains, expression of glycine-arginine with 36 repeats (GR36) was sufficient to cause NMD inhibition. In cells expressing GR36, stress granule accumulation was accompanied by decreased processing body formation, which contributed to the inhibition of NMD. Remarkably, expression of UPF1, a core gene in the NMD pathway, efficiently blocked neurotoxicity caused by arginine-rich dipeptide repeats in both cellular and *Drosophila* models. Although not as effective as UPF1, expression of another NMD gene UPF2 also ameliorated the degenerative phenotypes in dipeptide repeat-expressing flies, indicating that genetically reactivating the NMD pathway could suppress dipeptide repeat toxicity. Finally, after validating tranilast as an NMD-activating drug, we demonstrated the therapeutic potential of this asthma drug in cellular and *Drosophila* models of *C9orf72* dipeptide repeat neurotoxicity. Therefore, our study has revealed a cellular mechanism whereby arginine-rich C9orf72 dipeptide repeats could inhibit NMD activities by reducing the abundance of processing bodies. Furthermore, our results suggested that activation of the NMD pathway could be a potential therapeutic strategy for amyotrophic lateral sclerosis with defective RNA metabolism.

1 Institute of Neuroscience, State Key Laboratory of Neuroscience, Key Laboratory of Primate Neurobiology, Shanghai Institutes for Biological Sciences, Chinese Academy of Sciences, Shanghai 200031, China
2 University of Chinese Academy of Sciences, Shanghai 200031, China
3 Barrow Neurological Institute, Dignity Health, St. Joseph's Hospital and Medical Center, Phoenix AZ, 85013, USA
4 Shanghai Key Laboratory of Regulatory Biology, School of Life Sciences, East China Normal University, Shanghai, 200241, China

Correspondence to: Jin Xu, PhD
320 Yue Yang Road, Shanghai, China
E-mail: jin.xu@ion.ac.cn

Received September 3, 2018. Revised January 4, 2019. Accepted January 27, 2019. Advance Access publication April 1, 2019

Keywords: ALS; nonsense-mediated mRNA decay; *C9orf72*; dipeptide repeats; tranilast

Abbreviations: ALS = amyotrophic lateral sclerosis; DPR = dipeptide repeat; FTD = frontotemporal dementia; HRE = hexanucleotide repeat expansion; NMD = nonsense-mediated mRNA decay; P-body = processing body

Introduction

Amyotrophic lateral sclerosis (ALS) is a fast progressive, debilitating motor neuron disease with limited treatment options. There is no cure for the disease at present, and most commonly prescribed ALS drug—riluzole—can only prolong survival for a few months (Bensimon *et al.*, 1994). In 2017, a free-radical scavenger, edaravone, became the second FDA-approved ALS drug in more than 20 years after showing its benefits in slowing down disease progression (Abe *et al.*, 2017), even though the mode of action was not clear. Thus, there is a pressing need for disease-modifying therapeutic agents for ALS.

Although 90% of ALS cases are sporadic, advances in genetics have provided more clues for understanding the pathogenesis and offered new hope for treatments. The *C9orf72* hexanucleotide repeat expansion (HRE) is the most common cause of familial ALS and frontotemporal dementia (FTD), and accounts for >10% of sporadic ALS (DeJesus-Hernandez *et al.*, 2011; Renton *et al.*, 2011; Taylor *et al.*, 2016). Once the repeats reach more than 30–60, HRE becomes pathogenic (Gijselinck *et al.*, 2018). Current evidence suggests that three mechanisms may contribute to the development of *C9orf72* HRE-related ALS and FTD: dipeptide repeats (DPRs), abnormal RNA species, or reduced *C9orf72* gene expression (Gendron and Petrucelli, 2018). While the exact roles of HRE-derived RNA foci in disease progression remain to be clarified, accumulating evidence has suggested that DPRs are the more toxic products (Mizielinska *et al.*, 2014; Tao *et al.*, 2015; Tran *et al.*, 2015). The HRE produces five forms of DPRs via repeat-associated non-ATG translation (Ash *et al.* 2013; Mori *et al.*, 2013; Schludi *et al.*, 2015), and protein inclusions containing the DPRs are observed in the cerebellum, cortex, and hippocampus regions in *C9orf72* ALS patients (Mori *et al.*, 2013; Schludi *et al.*, 2015). Among these DPRs, the arginine-rich DPRs [poly proline-arginine (PR) and glycine-arginine (GR)] are important contributing factors of neurotoxicity (Kwon *et al.*, 2014; Mizielinska *et al.*, 2014; Tran *et al.*, 2015; Kanekura *et al.*, 2016; Zhang *et al.*, 2016). Besides arginine-rich DPRs, poly glycine-alanine (GA) may cause toxicity by modulating protein aggregation (May *et al.*, 2014; Zhang *et al.*, 2014, 2016; Lee *et al.*, 2017; Schludi *et al.*, 2017).

Recent evidence has shown that arginine-rich DPRs could also affect the formation of stress granules rich in RNA and RNA-binding proteins (RBPs) (Lee *et al.*, 2016; Boeynaems *et al.*, 2017; Green *et al.*, 2017; Li *et al.*, 2017; Cheng *et al.*, 2018; Zhang *et al.*, 2018*a*, *b*). Remarkably, several RBPs, including TDP-43, FUS, TAF15, EWSR1 and TIA1, have been genetically linked to ALS/FTD (Ling *et al.*, 2013; Mackenzie *et al.*, 2017). Furthermore, these proteins are also found in stress granules (Taylor *et al.*, 2016). Mutations in genes encoding these RBPs likely affect their functions and could cause dysregulation of RNA production, processing, transport, degradation and translation (Ling *et al.*, 2013; Taylor *et al.*, 2016; Mackenzie *et al.*, 2017). Therefore, dysfunction in RNA metabolism could be a common disease-causing mechanism in ALS/FTD (Ling *et al.*, 2013; Renton *et al.*, 2014; Taylor *et al.*, 2016). One of the pathways regulating mRNA abundance is nonsense-mediated mRNA decay (NMD), which was originally described as a quality control mechanism in eukaryotes to degrade defective mRNA with premature stop codon (He and Jacobson, 2015). Subsequently, NMD was found to regulate gene expression, especially of those genes with long 3′ untranslated regions (Lykke-Andersen and Jensen, 2015). The activation of the NMD pathway requires three conserved essential regulatory up-frame shift proteins (UPF1, UPF2, and UPF3) and the formation of a large protein complex to facilitate the cleavage of mRNA by endonucleases and exonucleases (Kervestin and Jacobson, 2012; He and Jacobson, 2015). Those key components of NMD machinery are found in processing bodies (P-bodies), which are membraneless ribonucleoprotein granules, rich in proteins, involved in RNA degradation (Sheth and Parker, 2006; Durand *et al.*, 2007; Parker and Sheth, 2007; Shukla and Parker, 2016; Hubstenberger *et al.*, 2017). Thus, P-bodies were considered as reservoirs for untranslated RNA and proteins regulating RNA decay, and could also be the site for NMD (Sheth and Parker, 2006; Durand *et al.*, 2007; Protter and Parker, 2016). Whether the NMD pathway is disturbed in ALS has never been carefully evaluated.

In this study, we investigated whether *C9orf72* HRE products could affect the NMD pathway. By coupling bioinformatic analysis of various transcriptome studies with validation experiments in multiple models of *C9orf72* HRE and DPRs, we found that *C9orf72* arginine-rich DPRs caused accumulation of transcripts normally degraded by the NMD pathway in patients and various models, suggesting the inhibition of NMD. Our cell biology studies revealed that the NMD inhibition is likely caused by decreased formation of P-bodies in cells expressing arginine-rich DPRs. More importantly, we have demonstrated in cellular and *Drosophila* models that reactivation of the NMD pathway by genetic and pharmacological approaches could rescue *C9orf72* arginine-rich DPR-induced neurotoxicity. Therefore, our results suggested that NMD pathway is a promising therapeutic target and an NMD-activating asthma drug—tranilast—could be a potential drug for ALS with dysfunctional RNA metabolism.

Materials and methods

Fly stocks

The UAS-DPRs transgenic flies were generous gifts of Dr Adrian Isaacs (Mizielinska *et al.*, 2014) (University College London). UAS-GFP-DPRs transgenic flies were described previously (Xu and Xu, 2018). $W^{[1118]}$ and $Elav^{C155}$-Gal4 were kind gifts from Dr Fude Huang (Shanghai Advanced Research Institute). w[*]; P{w[+mW.hs]=GawB}10D42, w*; P{UAS-Hsap\SNCA.A30P}40.1, w1118; P{UAS-HTT.128Q.FL}f27b, w*; P{tubP-GAL80ts}20; TM2/TM6B, Tb1, w*; P{UASp-GFP.Upf1}2, w*; P{UAS-Upf2.A}2, w*; P{UAS-Arc1.WT}3 and y1 v1; P{TRiP.JF01974}attP2 were obtained from Bloomington *Drosophila* Stock Center (BDSC). y1 v1; P{TRiP.GL01485}attP2 was the UAS-RNAi line used for knockdown of UPF1 under the control of Gal4. All flies were maintained at 24°C on a 12:12 h light:dark cycle at 60% humidity on a standard medium.

Plasmids

The G4C2 and DPR constructs were generous gifts of Dr Adrian Isaacs (Mizielinska *et al.*, 2014) (University College London). To generate GFP-tagged DPR constructs, untagged DPR constructs were subcloned into pEGFP-C1 vector. The flag-hUPF1 plasmid was generated by RT-PCR from the cDNA of SH-SY5Y cells and cloned into Flag-pcDNA3.1 vector. The coding sequence of DCP1α was amplified by RT-PCR from the cDNA of SH-SY5Y cells and cloned into pmCherry-C1 vector (modified based on pEGFP-C1). Dual luciferase NMD reporter was constructed as described (Boelz *et al.*, 2006; Keeling *et al.*, 2013). Briefly, the in-frame *Renilla* luciferase/β-globin fusion gene containing a premature stop codon in exon 2 (N39X) was generated by PCR mutagenesis and cloned into the psiCHECK-2 vector (Promega).

Climbing assay

Negative geotaxis behaviour was used to examine the fly mobility. Briefly, 10 male flies (aged 10 days) were transferred to the testing vials. Flies were tapped down to the bottom of the vials, and their climbing behaviour was video recorded. The height of each fly after 5 s was determined (Liu *et al.*, 2015). A total of three trials were performed for each vial, and the mean height for flies in each vial was calculated. At least three vials were used for each genotype.

Lifespan assay

For each group, 20 flies were collected 5 days after eclosion and transferred to a fresh vial. Every 5 days, the flies were moved to new vials with fresh food, and the number of dead flies was recorded. The survival rate for each group was calculated until the death of all flies.

Cell culture and transfection

Human neuroblastoma SH-SY5Y cells were cultured in Dulbecco's modified Eagle medium (DMEM; Life Technologies) with 10% foetal bovine serum (FBS; Life Technologies) and antibiotics, at 37°C with 5% CO_2. For quantitative PCR or NMD reporter analysis, cells were transfected with 3 μg GFP-GA36 or GFP-GR36 plasmids using Lipofectamine® 2000 reagent (Life Technologies) in 12-well plates. For immunostaining, cells were plated in 24-well plates and co-transfected with 0.5 μg GFP-GA36 or GFP-GR36 and 0.5 μg pcDNA3.1 or Flag-hUPF1 plasmids. The siRNA construct targeting UPF1 was transfected using Lipofectamine RNAiMAX (13778, Life Technologies). Cells were harvested 72 h after transfection for the subsequent studies. The sequence of siRNA was obtained from Mendell *et al.* (2004).

Stereotaxic injection of AAV-DPRs in mouse brain

Seven-week-old male wild-type C57BL/6 mice were purchased from SLAC Laboratory Animal Company. All animal experiments were approved and performed in accordance with the regulations by the Ethics and Animal Care and Use Committee of the Institute of Neuroscience, Shanghai Institutes for Biological Sciences. GFP-GA36 and GFP-GR36 were cloned into the adeno-associated virus (AAV) vector AOV-021 pAAV-CMV-MCS-3FLAG, and packaged by OBiO Inc with a titre of 6×10^{12}. Seven-week-old C57 mice were anaesthetized with pentobarbital sodium (80 mg/kg) and fixed on stereotaxic apparatus. AAV-GFP-GA36 and AAV-GFP-GR36 (1.5 μl) were injected into the hippocampus dentate gyrus (Bregma AP, −2.0 mm; ML, ±1.5 mm; DV, −1.9 mm) in the contralateral hemisphere. Mice were then maintained with proper food and water supply in a controlled environment. Five weeks post-injection, mice were either perfused intracardiacally with 4% paraformaldehyde for immune-fluorescent labelling or sacrificed for tissue collection and the subsequent quantitative PCR analysis.

Immunoprecipitation and immunoblotting

The procedures for immunoprecipitation and immunoblotting were described previously (Jiang *et al.*, 2018). Briefly, transfected SH-SY5Y cells (15 cm dish, 48 h after transfection) were lysed in NP-40 buffer with protease inhibitors. After centrifugation at 12 000 rpm for 15 min, 1 mg of protein lysates were precleaned with IgG for 1 h, followed by incubation with the control IgG or UPF1 antibody (1:50, ab109363, Abcam) overnight. After incubation with protein A/G sepharose beads (sc2003, Santa Cruz) for 1 h, the beads were washed and immunoprecipitated proteins were eluted by boiling in loading buffer, followed by western blot. Antibodies used in western blot included UPF1 antibody (1:3000, ab109363, Abcam), GFP antibody (1:3000, P30010, Abmart), DCP1α antibody (1:1000, H00055808-M06, Abnova), β-tubulin antibody (1:3000, M20005S, Abmart), GAPDH antibody (1:10 000, 60004–1, Proteintech) and HRP-conjugated secondary antibodies (Jackson lab).

Immunofluorescence

The mouse brains were dehydrated with 30% sucrose and embedded in optimum cutting temperature compound

(Tissue-Tek®). Frozen brains were then cryosectioned at a thickness of 40 µm. For SH-SY5Y cells, 48 h after transfection, the cells were fixed with 4% paraformaldehyde for 30 min. For flies, adult brains were dissected in phosphate-buffered saline (PBS) followed by 4% paraformaldehyde fixation for 30 min. The subsequent procedures were identical for all samples, with washes performed in PBST (0.3% Triton™ X-100 in PBS) followed by blocking and antibody incubation using PBST with 5% BSA as diluent. Primary antibodies used include: chicken anti-GFP (1:500, A10262, Thermo Fisher Scientific), mouse anti-NeuN, clone A60 (1:50, MAB377, Millipore), rabbit anti-Cleaved Caspase-3 (Asp175) (1:400, 9661 S, Cell Signaling Technology), mouse anti-LSM1 (1:50, TA503121, ORIGENE), mouse anti-DCP1α (1:50, H00055808-M06, Abnova), rabbit anti-PABP (1:200, ab21060, Abcam) and mouse anti-Flag (1:500, M20008L, AbMart). After primary antibody incubation at 4°C overnight, fluorescent labelled secondary antibodies (1:500, Thermo Fisher Scientific) were used for 2 h at room temperature. Finally, the slides were mounted in 70% glycerol. Images were acquired with Nikon A1 or Olympus FV10i confocal microscope and processed with Fiji software. Images were shown as maximum projection processing of multiple confocal scanning planes.

Quantitative PCR analysis

Fly heads, SH-SY5Y cells and mouse dentate gyrus were collected for various experiments and processed in TRIzol® reagent (Thermo Fisher Scientific) for RNA extraction. For quantitative PCR, 1 µg RNA was reverse transcribed (Takara), followed by PCR amplification with SYBR® green (CFX-connector, Bio-Rad). Gene expression data were calculated by the delta–delta Ct method. *Gadph* was used as reference control. The sequences of all the primers are available upon request.

Dual luciferase NMD reporter assays

GFP or GFP-tagged DPRs were co-transfected with the NMD reporter into SH-SY5Y cells for 48 h. Cells were collected and analysed following the instructions of dual-luciferase reporter assay system kit (E1910, Promega).

Drug treatment

Tranilast, nifulumic acid, febuxostat and nitazoxanide were purchased from Sigma-Aldrich and dissolved in DMSO at a concentration of 10 mM as stock solution. For SH-SY5Y cells, 24 h after transfection, chemicals were added to cell medium to the working concentration and incubated for 24 h, followed by washing with PBS and subsequent experiments. For flies, tranilast was added to the *Drosophila* food at the final concentration of 10 µM. The parent flies were removed after laying eggs on food. Embryo development was then analysed until death.

RNA sequencing

Four groups of flies [control PA36, (G4C2)36, PR36, UPF1-RNAi] were used for RNA-Seq. Each genotype contains two replicates with a total of 40 female fly heads. RNA was extracted by TRIzol® reagent (Thermo Fisher Scientific). Whole transcriptome libraries preparation and sequencing were performed by Annoroad Gene Technology Corporation. Whole transcriptome libraries were constructed by using NEB Next Ultra Directional RNA Library Prep Kit for Illumina (New England Biolabs) followed the manufacturer's instructions. The quality of the libraries was examined and quantified using the BioAnalyzer 2100 system (Agilent) and quantitative PCR (Kapa Biosystems). The resulting libraries were initially sequenced on a HiSeq X instrument (Illumina) and paired-end, 150-nucleotide reads were generated. Base calling was carried out using Illumina's real time analysis, and the raw sequence reads were exported in FASTQ format. The quality of the sequencing data was assessed by FastQC.

The FASTQ files containing raw sequence reads were aligned to fruit fly genome (BDGP6) by HISAT2 program (Version 2.1.o, default parameters). The number of reads mapped to each transcript were also calculated by HISAT2 (default parameters) based on the gene annotations from Ensembl Release 93 (www.ensembl.org). The read numbers were transcripts per kilobase million (TPM) from the HISAT2 result file. Compared with the control PA36 group, genes with P-value < 0.05 and |log2-transformed fold change| > 1 were considered as differentially expressed.

Biocomputational analysis

The raw reads count of transcriptome profiling in *C9orf72*-ALS and sporadic ALS were downloaded from the GEO database (GSE67196). DESeq (Anders and Huber, 2010) was applied to normalize the data and perform differential analysis. Using DESeq P-value < 0.05 and |log2-transformed fold change| > 1 as the cut-off, we identified 586 upregulated and 41 downregulated genes in the cerebellum, 389 upregulated and 44 downregulated genes in the frontal cortex.

The differentially expressed genes in UPF1/2/3-deficient cells were directly extracted from the supplementary tables of the corresponding papers (Mendell *et al.*, 2004; Wittmann *et al.*, 2006; Nguyen *et al.*, 2012).

Statistical analysis

Data analysis and statistics were carried out using GraphPad Prism 7 (GraphPad Software Inc., San Diego, CA) and are detailed in the figure legends. $P < 0.05$ was considered as a significant change.

Data availability

Differentially expressed genes are listed in Supplementary Tables 4–6. The raw RNA-Seq data have been uploaded to GEO (GSE123172). All the other materials are available upon request.

Results

Inhibition of nonsense-mediated mRNA decay pathway in *C9orf72* patients

To evaluate whether the NMD pathway could be disturbed in patients with *C9orf72* HRE, we first conducted unbiased

bioinformatics analysis to compare published transcriptome datasets from various *C9orf72* ALS-related sources with those from human cells with defective NMD pathways. *C9orf72* ALS-related samples included brain tissues from ALS patients ($n = 8$ *C9orf72* ALS and $n = 10$ sporadic ALS) (Prudencio *et al.*, 2015), motor neurons collected from eight *C9orf72* ALS patients using laser-guided microdissection (Cooper-Knock *et al.*, 2015) and induced pluripotent stem cell (iPSC)-derived motor neurons from two *C9orf72* ALS patients (Shi *et al.*, 2018). The available NMD-defective transcriptome datasets were from studies using cells deficient of the essential components of the NMD pathway, including lymphocytes from five patients with UPF3B/NMD deficiency (Nguyen *et al.*, 2012) and HeLa cells with depleted UPF1 or UPF2 (Mendell *et al.*, 2004; Wittmann *et al.*, 2006). It is worth noting that UPF3B/NMD-deficient patients exhibited a variety of neuropsychiatric defects, including intellectual disability (Nguyen *et al.*, 2012). We found that there were a significant number of overlapping genes between the *C9orf72* ALS cerebellum tissues and each human cell type with defective NMD functions (Fig. 1A–C and Supplementary Table 1), especially the primary lymphocytes from *UPF3B*$^{-/-}$ patients. Gene ontology analysis showed that stress response and immune system-related genes were significantly enriched among the overlapping genes (Supplementary Table 2). Similarly, we have observed a significant number of overlapping genes between NMD-defective cells and *C9orf72*-patient-derived iPSC motor neurons (Fig. 1D–F) or microdissected motor neurons from *C9orf72* patient spinal cord (Supplementary Fig. 1A). In every pair of compared groups, we observed essentially no overlapping downregulated genes, and none of the downregulated genes in *C9orf72* ALS brains are NMD substrate genes. Since even UPF1/UPF2/UPF3-deficient cells only showed a few (< 6) commonly upregulated genes in pair-wise comparison (Wittmann *et al.*, 2006; Nguyen *et al.*, 2012), our results strongly suggested that *C9orf72* HRE products could cause the accumulation of mRNA species regulated by NMD in *C9orf72* patients. We also compared the transcriptome of the sporadic ALS brain tissues with that of UPF3B/NMD lymphocytes and UPF1/2-deficient cells and found a much lower number of overlapped upregulated genes (Supplementary Fig. 2), suggesting that the accumulation of NMD-regulated mRNA was an effect specifically related to *C9orf72* products.

Arginine-containing *C9orf72* dipeptide repeats inhibit the nonsense-mediated mRNA decay pathway

Given the lead from the bioinformatic analysis, we used the *Drosophila* model to assess whether *C9orf72* GGGGCC (G4C2) HRE products could affect the expression of NMD-regulated genes *in vivo* by RNA-seq analysis. As multiple studies have shown that the arginine-rich DPRs generated from the HRE are the more toxic species (Mizielinska *et al.*, 2014; Tao *et al.*, 2015; Tran *et al.*, 2015), we examined the effects of both G4C2 HRE and proline-arginine dipeptide with 36 repeats (PR36) on NMD-regulated gene expression in *Drosophila*. We chose flies with pan-neuronal expression of PR36 because we have found previously that flies expressing glycine-arginine (GR36) could not survive beyond the pupa stage (Xu and Xu, 2018). We compared the brain transcriptome data from 5-day-old flies expressing (G4C2)36 (Supplementary Table 4) or PR36 (Supplementary Table 5) with those from flies with defective NMD pathways caused by deficient UPF1 (Supplementary Table 6) or defective UPF2. UPF1 deficiency was achieved by pan-neuronal expression of the UAS-UPF1 RNAi, and the RNA-seq data from UPF2-haploinsufficiency flies were retrieved from a previous study (Chapin *et al.*, 2014). Flies expressing non-toxic proline-alanine 36 (PA36) (Xu and Xu, 2018) were used as control. In (G4C2)36-expressing flies, the expression of 337 genes showed increase (fold change > 2, $P < 0.05$). Among those upregulated genes, 66 genes were also found to be accumulated in UPF1-knockdown flies (Fig. 1G) ($P = 3.19 \times 10^{-35}$), suggesting that the accumulation of NMD-regulated genes observed in human tissues (Fig. 1A–F) could also be recapitulated in the *Drosophila* model. Interestingly, no statistically significant overlap was found between (G4C2)36-expressing flies and UPF2 mutant flies ($P = 0.6705$) (Supplementary Fig. 1B), suggesting that the UPF1 function could be more vulnerable to *C9orf72* HRE toxicity than UPF2 function in flies. We then assessed the effects of PR36 and found that 67 of the 275 upregulated genes caused by PR36 expression were also accumulated in flies with UPF1 deficiency ($P = 3.63 \times 10^{-42}$) (Fig. 1H). Furthermore, 19 common genes were identified between PR36-expressing flies and UPF2 mutant flies ($P = 0.0182$) (Supplementary Fig. 1C). Notably, among the two groups of genes commonly accumulated in UPF1-deficient flies and (G4C2)36- or PR36-expressing flies, 36% of them are identical (Fig. 1I) ($P = 4.55 \times 10^{-16}$), indicating that arginine-rich DPRs, such as PR, could effectively affect the NMD pathway and could be the main contributors to NMD inhibition by *C9orf72* HRE. Because of this discovery, we focused on the inhibition of NMD mainly by DPRs in our subsequent studies.

To validate the observations from transcriptomic studies, we examined the expression of four NMD substrates (*Sin3A*, *Gadd45*, *Xrp1* and *Arc1*) (Giorgi *et al.*, 2007; Bramham *et al.*, 2008; Chapin *et al.*, 2014; Nelson *et al.*, 2016) in PR36-expressing flies and UPF1-deficient flies, as well as in flies expressing GFP-tagged GR36, which has lower toxicity than untagged GR36, but comparable toxicity to PR36 (Xu and Xu, 2018) (Fig. 1J). Those four selected genes were among the seven validated NMD substrates that were upregulated in both UPF1-deficient and UPF2 mutant flies (Supplementary Table 3), and have well-characterized functions such as stress response

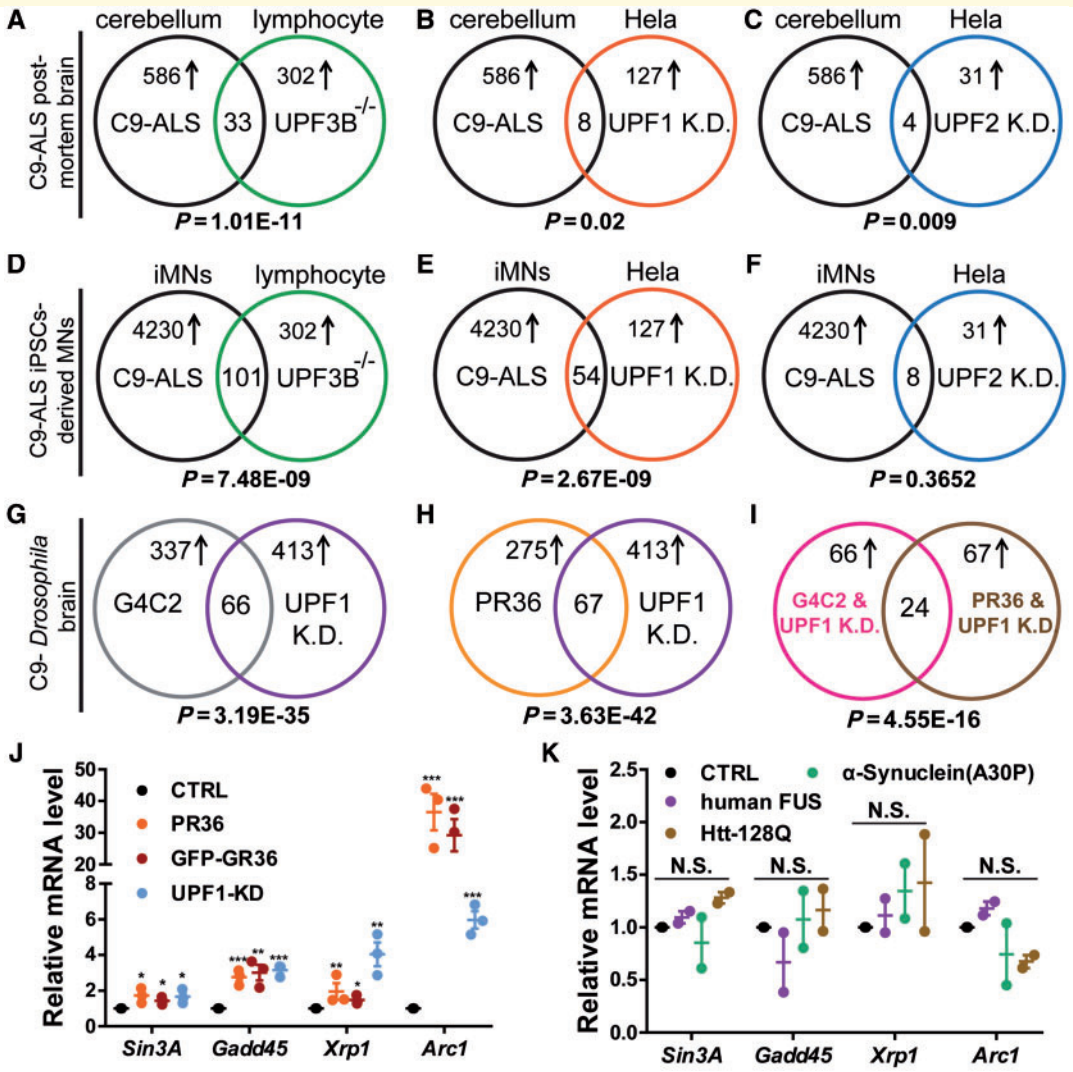

Figure 1 NMD targeted genes are accumulated in C9orf72-ALS brains, iPSC-derived motor neurons and flies expressing C9orf72 HRE products. (**A**–**F**) Venn diagrams showing the number of common transcripts between the C9orf72-ALS cerebellum (*top* row) or iPSC-derived motor neurons (iMNs, *middle* row) and the lymphocytes from UPF3B-deficient patients (**A** and **D**), or UPF1 (**B** and **E**), UPF2 (**C** and **F**) knockdown HeLa cells. (**G** and **H**) Venn diagrams showing the number of common upregulated transcripts between fly brains expressing (G4C2)36 (**G**) or PR36 (**H**) and fly brains with UPF1 knockdown (UPF1 K.D.). (**I**) Venn diagram showing the number of overlapping transcripts between upregulated genes from **G** and **H**. The *P*-value under each diagram indicates the statistical significance (by Fisher's exact test) for the number of the overlapping genes from each group. (**J**) Validation of indicated NMD targets in female flies expressing PR36, GFP-GR36, or UPF1 RNAi. Mean ± standard error of mean (SEM), $n = 3$ independent experiments, two-tailed Student's *t*-test, $^{*}P < 0.05$, $^{**}P < 0.01$, $^{***}P < 0.005$. CTRL genotype = ElavC155/+ . (**K**) The relative abundance of indicated NMD targets in female flies with pan-neuronal expression of α-synuclein with the A30P mutation, huntingtin with 128 polyQ repeats, wild-type human FUS. As neuronal expression of FUS caused pupal lethality, to obtain viable adult flies, temperature-sensitive Gal80 was used to specifically drive the FUS expression at the adult stage. Mean ± SEM, $n = 2$ independent experiments, two-tailed Student's *t*-test, N.S. = no significance.

(Fornace *et al.*, 1992) and synaptic regulation (Bramham *et al.*, 2008). Consistent with the RNA-seq results, those four genes were upregulated in both PR36- and GFP-GR36-expressing flies, indicating inhibition of the NMD pathway as a common feature for arginine-rich DPRs (Fig. 1J). In contrast, other known neurotoxic proteins, such as Parkinson's disease-causing A30P α-synuclein, Huntington's disease-causing huntingtin poly-glutamine with 128 repeats (128Q), and another ALS/FTD-associated protein FUS, did not significantly affect the expression of these genes (Fig. 1K), suggesting that the upregulation of NMD targets *Sin3A*, *Gadd45*, *Xrp1* and *Arc1* is likely to be specific for *C9orf72* arginine-rich DPRs. Taken together, the expression of *C9orf72* arginine-rich DPRs likely causes the suppression of NMD in *Drosophila*.

To directly assess the effects of DPRs on NMD activity, we made a luciferase reporter gene fused to the β-globin gene with a premature stop codon, a standard paradigm for

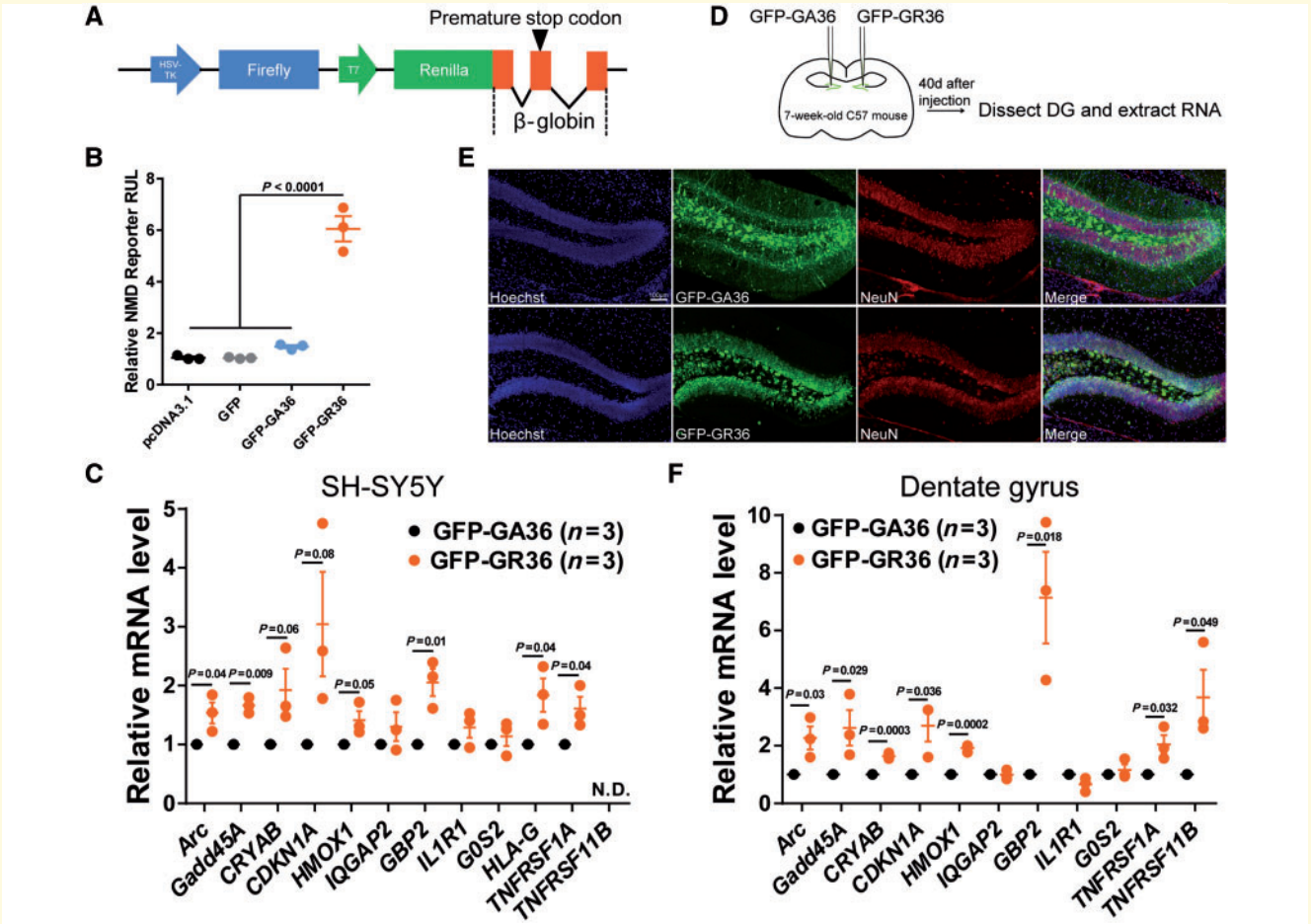

Figure 2 NMD pathway is inhibited in GFP-GR36-expressing human cells and mouse brains. (**A**) Schematic representation of the dual luciferase NMD reporter. The firefly luciferase was used as transfection efficiency control, whereas the renilla luciferase fused to a human β-globin with a premature stop codon mutation (N39X) was used to monitor the NMD pathway activity. (**B**) GFP-GR36 impaired the NMD function and led to the accumulation of an NMD reporter. Indicated constructs were co-transfected with the NMD reporter into SH-SY5Y cells. Mean ± SEM, *n* = 3 independent experiments, one-way ANOVA followed by Tukey's multiple comparison tests. (**C**) The mRNA levels of common NMD targets upregulated in C9orf72-ALS patients' cerebellum and frontal cortex (highlighted in Supplementary Table 1) were also increased in the human SH-SY5Y cells transfected with GFP-GR36, *n* = 3 independent experiments. Mean ± SEM, two-tailed Student's *t*-test. TNFRSF11B was not detected (N.D.) due to its low expression in SH-SY5Y cells. (**D**) Schematic depiction of the experimental design. AAV expressing GFP-GA36 or GFP-GR36 was separately injected to the dentate gyrus (DG) in the contralateral hemispheres, and the tissues were collected 5 weeks after injection for mRNA analysis. (**E**) Representative images showing the robust expression of GFP-GA36 or GFP-GR36 in dentate gyrus. (**F**) Relative mRNA levels of the same genes as in **C** in AAV-GFP-GA36/GR36-injected animals. *n* = 3 male mice. Mean ± SEM, two-tailed Student's *t*-test.

evaluating NMD activity (Boelz *et al.*, 2006; Keeling *et al.*, 2013) (Fig. 2A). The validity of the reporter was confirmed by increased reporter activity in cells with silenced UPF1 expression (Supplementary Fig. 3A and B). We found that GFP-GR36 expression elevated the NMD reporter gene expression by 5-fold in the human SH-SY5Y cell line (Fig. 2B). In contrast, control GFP or GFP-GA36 expression led to very little change in NMD reporter expression (Fig. 2B).

We have shown that arginine-rich DPRs were the main contributors to NMD inhibition by G4C2 repeats in *Drosophila* (Fig. 1G–I). To validate this conclusion in mammalian cells, we selected a group of overlapping genes from *C9orf72* ALS brain with G4C2 repeats and NMD-deficient cells (Fig. 1A–F) and tested their expression in a human neuroblastoma cell line or in mouse brain expressing only the DPRs. Those selected genes also met our criteria to be expressed in both cerebellum and frontal cortex (Supplementary Table 1). In addition, the mammalian *Arc1* homologue *Arc* and *Gadd45*, a stress-related gene, was also included as it was upregulated by poly PR/GR in *Drosophila*. The expression of most of those genes was significantly higher in human SH-SY5Y cells expressing GFP-GR36 than in cells expressing GFP-GA36 (Fig. 2C), and were further validated as NMD-regulated genes in cells with UPF1 silencing

(Supplementary Fig. 3C). Moreover, we performed an *in vivo* assessment by injecting AAV-GFP-GR36 or control AAV-GFP-GA36 into the mouse dentate gyrus (Fig. 2D and E) and found that the expression of NMD target genes was mostly higher in the mouse brain expressing GFP-GR36 than in those expressing GFP-GA36 (Fig. 2F). These results demonstrate that the suppression of NMD by arginine-rich DPRs was conserved across species.

Reduced processing body formation in *C9orf72* dipeptide repeat expressing cells contributes to NMD suppression

We then attempted to investigate the potential mechanism that could account for the NMD inhibition by *C9orf72* DPRs. We excluded the possibility that arginine-rich DPRs could form a complex with UPF1 (Supplementary Fig. 4A) or affect the expression of UPF genes (Supplementary Fig. 4B and C). As P-bodies are ribonucleoprotein granules harbouring proteins participating in NMD, and could be the sites for NMD (Sheth and Parker, 2006; Durand *et al.*, 2007; Protter and Parker, 2016; Hubstenberger *et al.*, 2017), we examined the abundance of P-bodies by immunofluorescence labelling of endogenous specific P-body markers DCP1α (Fig. 3A) or LSM1 (Supplementary Fig. 5A) in cells transfected with GFP-GR36 or control GFP or GFP-GA36. The number of DCP1α or LSM1-positive P-bodies was significantly reduced in cells expressing GFP-GR36 (Fig. 3B and Supplementary Fig. 5B), and this effect was not due to decreased expression of the marker protein DCP1α (Supplementary Fig. 5C and D).

Given that stress granules and P-bodies are related ribonucleoprotein granules with some shared components (Kedersha *et al.*, 2005; Durand *et al.*, 2007; Protter and Parker, 2016; Youn *et al.*, 2018), we assessed whether the decreased abundance of P-bodies was related to increased stress granules formed in cells expressing GFP-GR36 (Fig. 3C and Supplementary Fig. 5E). We examined the DCP1α-positive P-bodies in GFP-GR36-expressing cells with (SG+) or without (SG−) stress granules (Fig. 3C) and found that the abundance of P-bodies was significantly lower in cells with stress granules (Fig. 3D). As P-bodies and stress granules are dynamically linked (Kedersha *et al.*, 2005), our results suggested that increased stress granule formation in cells expressing arginine-rich DPRs could simultaneously contribute to the loss of P-bodies.

We found overexpression of a specific P-body component decapping enzyme DCP1α could lead to increased abundance of P-bodies as determined by labelling endogenous LSM1 (Fig. 3E). Therefore, we assessed whether the inhibition of NMD could be rescued by overexpressing DCP1α. Using the NMD reporter construct, we found that DCP1α could alleviate the suppression of NMD activity by GFP-GR36 (Fig. 3F). Taken together, *C9orf72* arginine-rich DPRs could suppress NMD by decreasing the abundance of P-body formation, which is likely influenced by concurrent increase of stress granules.

Activation of NMD protects against *C9orf72* dipeptide repeat neurotoxicity

We then tested whether the activation of NMD may prevent *C9orf72* DPR-induced toxicity. As UPF1 is a key protein initiating NMD, we co-transfected UPF1 with control GFP, GFP-GA36 or GFP-GR36 in human SH-SY5Y cells and assessed the number of cells with apoptosis marker activated caspase-3. UPF1 expression did not affect the abundance of co-transfected GFP-GR36 (Supplementary Fig. 6). While GFP-GR36 led to a great increase of activated caspase-3, co-expression of UPF1 completely prevented the apoptotic cell death (Fig. 4). Similarly, UPF1 effectively protected against (G4C2)36-caused apoptosis (Supplementary Fig. 7).

The protective role of UPF1 was also evident in *Drosophila*. First, knockdown of UPF1 with siRNA led to impaired motor function (Supplementary Fig. 8). Second, UPF1 was able to reverse the build-up of four NMD substrates (Fig. 1J and Supplementary Fig. 9A) and effectively rescued the loss of motor neurons and axon projection by PR36 (Fig. 5A–C and Supplementary Fig. 10). Finally, overexpression of UPF1 or UPF2 also rescued GFP-GR36-induced motor deficits and shortened lifespan (Fig. 5D and E). It is worth noting that UPF1 exhibited a much stronger rescue effect than UPF2, consistent with our earlier observation that UPF1 could be more susceptible to DPR toxicity (Fig. 1H and Supplementary Fig. 2C). One caveat in the lifespan study is that the UPF1 and UPF2 flies were not backcrossed for more than six generations. Regardless, our data strongly suggest that the restoration of the NMD activity by increasing the expression of core genes in the NMD pathway could alleviate neurotoxicity induced by arginine-rich DPRs.

Next, we aimed to test whether compounds activating NMD could be effective therapeutics in *C9orf72* ALS models. In a previous study investigating the effects of NMD inhibitors, a short list of compounds that could activate NMD were identified using a dual-colour, bioluminescence-based screening assay (Nickless *et al.*, 2014). We acquired four of the compounds (tranilast, nifulumic acid, febuxostat and nitazoxanide), and carried out validation assays to further confirm their NMD-activating effects using our β-globin-based NMD reporter (Fig. 2A) in human SH-SY5Y cells expressing *C9orf72* DPRs. Surprisingly, we found that only tranilast demonstrated the activity consistent with the features of an NMD activator, exhibiting dose-dependent degradation of the NMD reporter (Fig. 6A), while not affecting PR expression (Supplementary Fig. 11). In contrast, nifulumic acid had

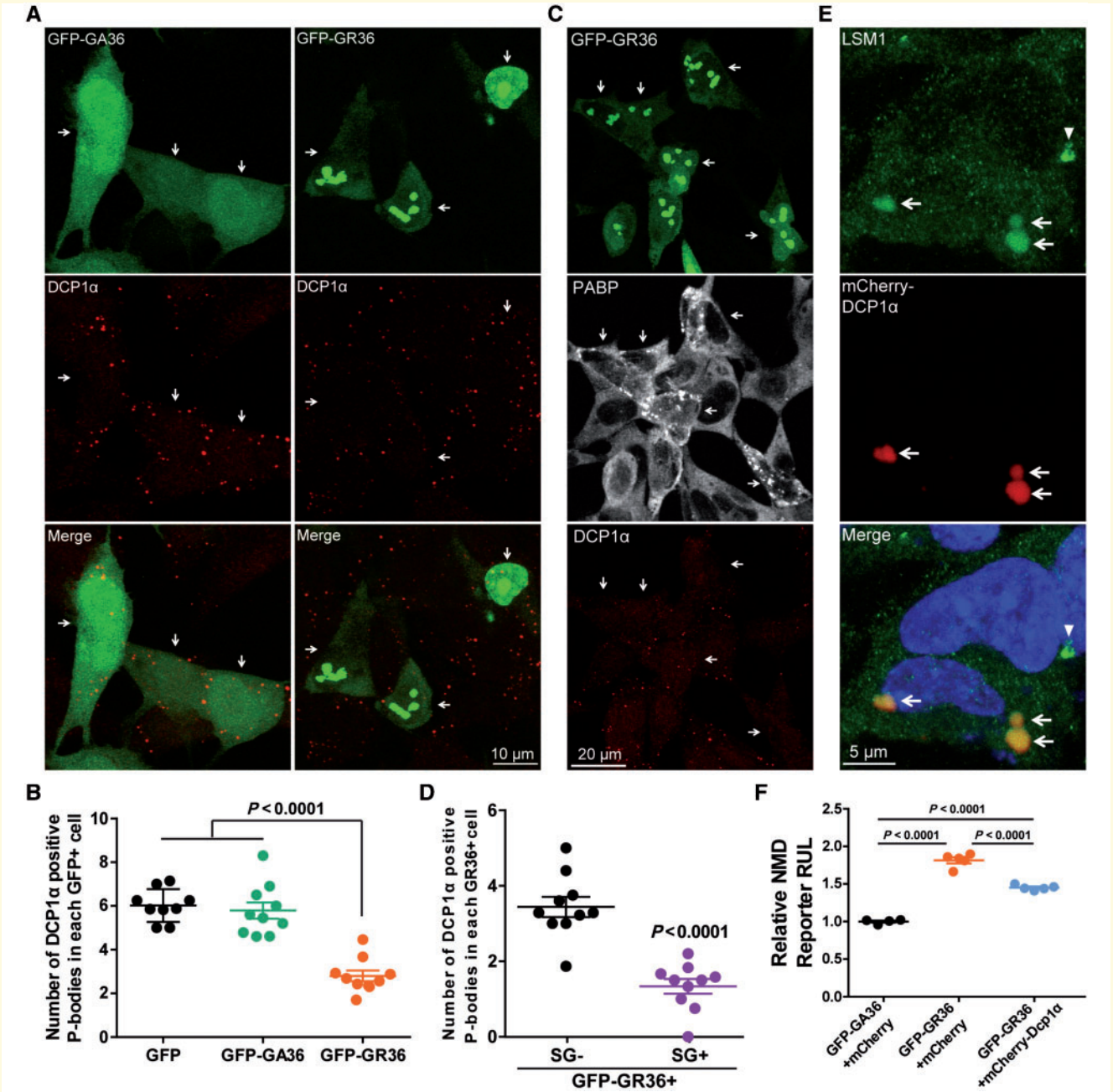

Figure 3 Decreased P-body formation in GFP-GR36-expressing cells leads to NMD inhibition. (**A**) Representative images showing the DCP1α-positive P-bodies in GFP-GA36 or GFP-GR36-expressing cells. Arrows indicate GFP+ cells. (**B**) Quantification of the abundance of DCP1α-positive P-bodies per GFP+ cell. Mean ± SEM, one-way ANOVA followed by Tukey's multiple comparison tests. n = 9–10 fields, each with at least 15 GFP+ cells. (**C**) Representative images showing the DCP1α-positive P-bodies and stress granules in GFP-GR36-expressing cells. Arrows indicate GFP-GR36+ cells containing stress granules. (**D**) Quantification of the abundance of DCP1α-positive P-bodies in GFP-GR36-expressing cell with (SG+) or without (SG−) stress granules. Mean ± SEM, two-tailed Student's t-test. Each dot represents the average number of P-bodies in one field, n = 118 SG− cells and n = 56 SG+ cells were scored. (**E**) Representative pictures showing DCP1α overexpression increasing LSM1+ P-bodies. The P-bodies in cells with or without mCherry-DCP1α expression were indicated by arrows or arrowhead, respectively. (**F**) NMD reporter activity in cells with indicated transfection condition. Mean ± SEM, one-way ANOVA followed by Tukey's multiple comparison tests, n = 4–5 biological replicates.

no effect, whereas febuxostat and nitazoxanide exhibited inhibition of NMD in our reporter system (Supplementary Fig. 12). Based on these results, we chose tranilast for our subsequent studies to evaluate its therapeutic potential.

In human SH-SY5Y cells, tranilast could efficiently reactivate NMD activity as demonstrated by reduced expression of NMD reporter at a dose as low as 2.5 μM (Fig. 6A), and it could effectively suppress GFP-GR36 or

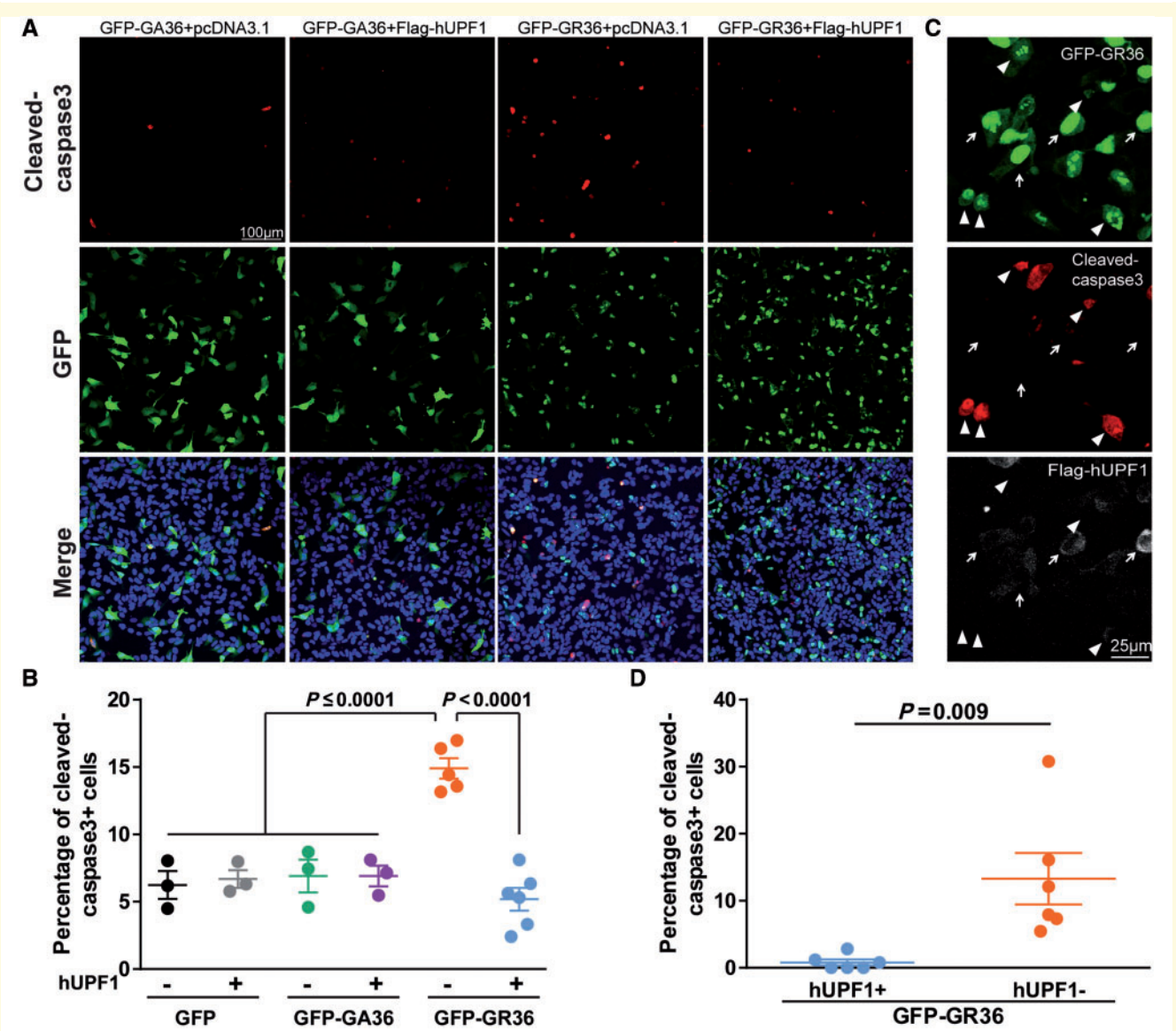

Figure 4 UPF1 completely blocks GFP-GR36-induced toxicity in SH-SY5Y cells. (**A**) Representative images showing the suppression of caspase-3 activation by hUPF1 in SH-SY5Y cells expressing GFP-GR36. Cells were co-transfected with GFP-GR36 and pcDNA3.1 or UPF1, and quadruple-labelled for GFP, activated caspase-3, UPF1 (not shown) and DAPI for analysis. (**B**) Quantification of cells with cleaved caspase-3 in each group. Images acquired under 20× objective were compiled and quantified blindly. The expression of GFP-DPRs was not changed by hUPF1 overexpression (data not shown). Values represent mean ± SEM, one-way ANOVA followed by Tukey's multiple comparison tests, n = 3–6 fields, each with at least 100 cells per field. (**C** and **D**) Representative images showing the effect of UPF1 on GFP-GR36 toxicity in the same cell population. As not all the co-transfected cells expressed both GFP-GR36 and UPF1, the activated caspase-3 signals were analysed based on the presence (indicated by arrows) and absence (indicated by arrowheads) of UPF1 in GFP-GR36-expressing cells. The quantification is shown in **D**. Mean ± SEM two-tailed Student's t-test. n = 6 fields with at least 130 cells each.

(G4C2)36-induced apoptosis (Fig. 6B and C and Supplementary Figs 13 and 14). *In vivo*, tranilast feeding starting at the larval stage led to suppressed expression of NMD substrates *Arc1*, *Gadd45* and *Xrp1*, which were significantly induced in flies expressing PR36 (Fig. 6D). While GR36 expression in *Drosophila* caused a reduction in the number of pupae formed and significantly decreased pupa-to-adult viability, treatment with 10 μM tranilast improved the survival of GR36-expressing flies (Table 1). The female pupa-to-adult viability in the tranilast-treated GR36 group rose from 10–15% to >40%. In flies expressing the less toxic GFP-GR36, tranilast treatment led to a significant increase in the number of pupae formed (from mid-20 s to 56). Furthermore, a small number of male flies expressing GFP-GR36 could survive to the adult stage with tranilast feeding (Table 1). Finally, tranilast significantly improved the adult survival rate (Fig. 6E) and motor function (Fig. 6F) in flies expressing either PR36 or GFP-GR36.

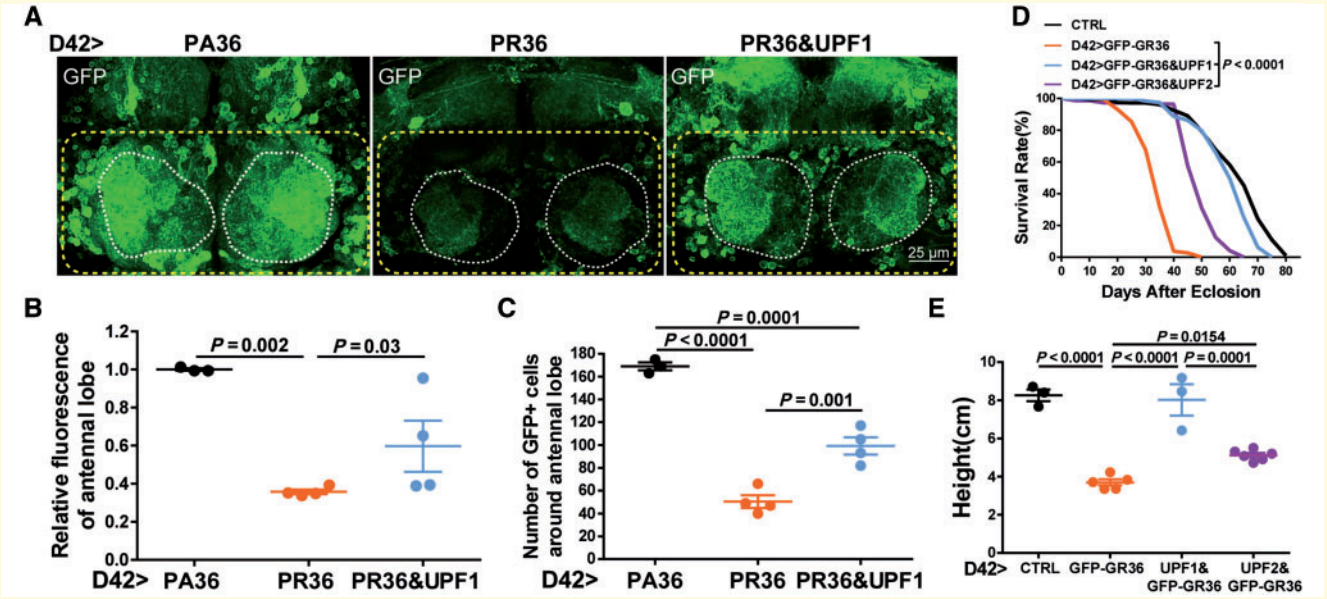

Figure 5 Expression of core genes in the NMD pathway ameliorates DPR-induced neurodegeneration in flies. (**A**–**C**) Representative images showing the cell body and axonal projection of motor neurons with indicated genotype at the age of 30 days. As reliable antibodies for *Drosophila* motor neurons were not available, D42 > mCD8::GFP was used to label motor neuron population. White-dotted circles indicate antennal lobe, a neuropil of motor neurons. The relative fluorescent intensity of antennal lobe is shown in **B**. As most of the motor neurons are surrounding the antennal lobe, GFP-positive neurons within yellow-dotted rectangles were quantified (**C**). All the images were taken under identical parameters including the equivalent value of laser intensity, gain, off-set and pinhole. Each dot represents the result from one different male fly. The expression of PR36 was not affected by UPF1 overexpression (data not shown). Mean ± SEM, one-way ANOVA followed by Tukey's multiple comparison tests. (**D**) Expression of UPF1 or UPF2 in motor neurons prolonged the life span of GFP-GR36-expressing flies. Log-rank test, each genotype includes n = 120 male flies in six vials. (**E**) Over-expression of UPF1 or UPF2 in motor neurons rescued the GFP-GR36-caused climbing defect. Male, mean ± SEM, $n \geqslant 3$ tubes, each dot represents the result from one vial of flies, one-way ANOVA followed by Tukey's multiple comparison tests.

Thus, NMD-activating compound tranilast could protect against the neurotoxicity induced by *C9orf72* DPRs in human cells and *Drosophila*.

Discussion

By combining transcriptome analysis of tissues and cells from *C9orf72* patients with experimental validation in various models, we have found that *C9orf72* HRE products, especially the arginine-rich DPRs could inhibit the NMD pathway, potentially by suppressing the formation of P-bodies. Remarkably, reactivation of the NMD pathway could protect against the neurotoxicity caused by G4C2 expansion repeat products and therefore could be a promising therapeutic approach for ALS. Furthermore, we have suggested tranilast, an NMD-activating drug with good safety record, as a potential therapeutic agent for ALS.

Proper surveillance of various RNA species to remove faulty and excess RNA in the cells is vital for the survival and thriving of the organism. A major surveillance mechanism is the NMD pathway, which selectively targets mRNAs with premature termination codon or long 3′ untranslated region for degradation (He and Jacobson, 2015; Lykke-Andersen and Jensen, 2015). Because of its importance, the roles of NMD in human diseases, and even ageing and longevity, have been increasingly recognized (Bhuvanagiri *et al.*, 2010; Son *et al.*, 2017; Tabrez *et al.*, 2017; Popp and Maquat, 2018). Interestingly, Connolly (2005) proposed a hypothesis that the translation of normally untranslated nonsense RNA due to a faulty surveillance system may contribute to the accumulation of misfolded protein and lead to neurodegeneration. However, there has been no direct evidence to connect the suppression of the NMD pathway to neurodegenerative diseases. For FTD-associated progranulin, mutations that cause a frameshift and premature termination codon actually stimulated the degradation of progranulin mRNA via NMD (Skoglund *et al.*, 2009; Nguyen *et al.*, 2018). Our current study revealed that the inhibition of NMD could be one of the major consequences in *C9orf72* ALS. Since ~40% of alternative spliced transcripts could generate premature stop codons and NMD is coupled to remove those defective mRNAs (Lewis *et al.*, 2003; Tabrez *et al.*, 2017), the suppression of NMD could have likely contributed to the extensive alternative splicing and polyadenylation defects seen in the *C9orf72* brains (Prudencio *et al.*, 2015). Besides the build-up of aberrantly spliced transcripts,

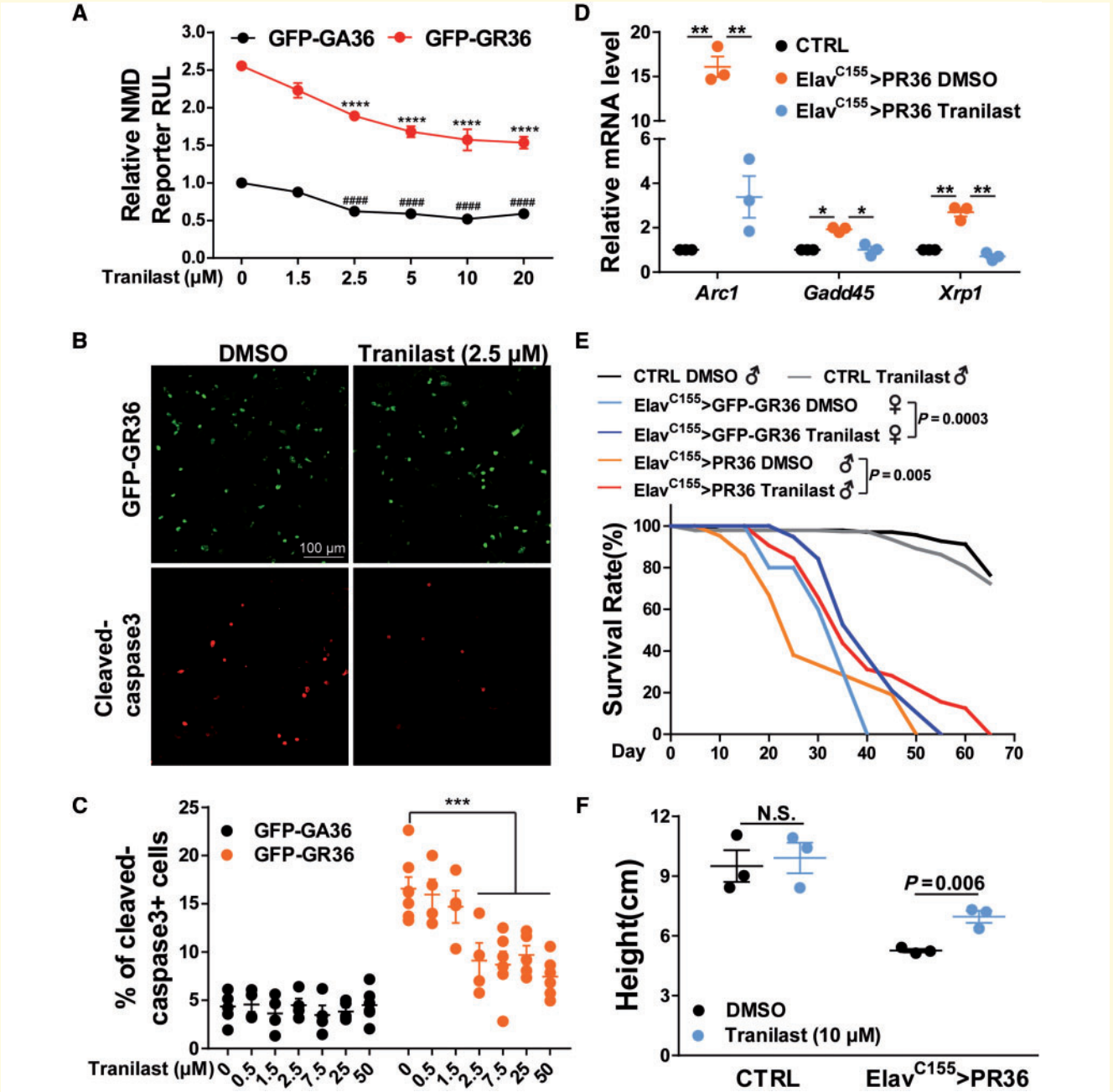

Figure 6 Tranilast, an NMD activator, ameliorates GR/PR toxicity in SH-SY5Y cells and flies. (**A**) The dose effect of tranilast on an NMD reporter in GFP-GA36 or GFP-GR36-transfected cells. Mean ± SEM, $n = 3$ independent experiments. Asterisks or hash symbols represents the statistically significant differences of luciferase activities between cells treated with indicated dosage and untreated control in GFP-GR36 group or GFP-GA36 group. One-way ANOVA followed by Tukey's multiple comparison tests, ****, #### $P < 0.0001$. (**B** and **C**) Representative images showing the protective effects of 2.5 μM of tranilast on GFP-GR36-induced caspase3 cleavage. Quantification was shown in **C**. Mean ± SEM, two-way ANOVA, ***$P < 0.005$, $n = 3$–6 fields, with at least 100 cells per field. The protective effects of tranilast at the dosage of 2.5 and 7.5 μM were confirmed in two more replicate experiments. (**D**) The mRNA abundance of *Arc1, Gadd45* and *Xrp1* in the brains of 5-day-old female flies treated with DMSO or tranilast. Mean ± SEM, $n = 3$ independent experiments, one-way ANOVA followed by Tukey's multiple comparison tests. *$P < 0.05$, **$P < 0.01$. (**E**) Feeding flies with 10 μM tranilast from larval stage prolonged the lifespan in GFP-GR36 or PR36-expressing flies. Log-rank test, each genotype includes $n = 80$ flies in four vials. As ElavC155 > GFP-GR36 expression in male is lethal, female flies were used for lifespan assay. (**F**) Tranilast treatment improved the mobility in PR36-expressing flies. The expression of PR36 was not affected by tranilast (data not shown). Male, mean ± SEM, $n = 3$ tubes, each dot represents the result from one vial of flies, two-tailed Student's *t*-test. CTRL genotype = ElavC155/+; ♀ = female; ♂ = male.

Table 1 Tranilast treatment from embryo stage partially rescues GR36- or GFP-GR36-caused developmental defects

	Treatment	Pupae formation	Pupae-to-adult viability (%)
$Elav^{C155}$-Gal4 × UAS-GR36	CTRL	27	Male lethal Female 3/27 (11.1)
	0.1% DMSO	28	Male lethal Female 4/28 (14.3)
	10 μM Tranilast	32	Male lethal **Female 13/32 (40.6)**
$Elav^{C155}$-Gal4 × UAS-GFP-GR36	CTRL	27	Male lethal Female 10/27 (37)
	0.1% DMSO	23	Male lethal Female 10/23 (43.5)
	10 μM Tranilast	**56**	**Male 3/56 (5.4)** **Female 23/56 (41.1)**

The numbers of pupae and viable adults with indicated genotype and treatment were listed. Bold indicates the beneficial effects. CTRL = control; DMSO = dimethyl sulphoxide.

accumulation of some key NMD substrates could also be detrimental. Two of the well known NMD targets identified in GR/PR-expressing flies, Arc1 and Gadd45 (Fig. 1J), could contribute to DPR-induced neurotoxicity. Gadd45 has been shown to cause neurodegeneration in flies, and its degradation via NMD is essential for the viability (Nelson *et al.*, 2016). In our study, we found that Arc1 partially mediated DPR neurotoxicity in flies (Supplementary Fig. 15). Therefore, the suppression of the NMD pathway would cause a broad impact in neuronal survival by increasing the expression of a variety of target genes.

We have found that the inhibition of NMD by the *C9orf72* HRE products was mainly mediated by arginine-rich DPRs, which could increase cellular stress and promote the formation of stress granules while suppressing protein translation (Lee *et al.*, 2016; Boeynaems *et al.*, 2017; Green *et al.*, 2017; Li *et al.*, 2017; Cheng *et al.*, 2018; Zhang *et al.*, 2018*a*, *b*). In this report, we found that the formation of P-bodies was also suppressed by arginine-rich DPRs, thus contributing to the inhibition of NMD. This observation extends our understanding of the impact of DPRs on various ribonucleoprotein granules. Interestingly, the reduced abundance of P-bodies was accompanied by increased formation of stress granules in the same cell. As stress granules and P-bodies are dynamically linked (Kedersha *et al.*, 2005; Protter and Parker, 2016), it is conceivable that dynamic stress granule formation may drain the components from P-bodies and lead to the disintegration of P-bodies. Given that poly GR/PR could interact with some RNA-binding proteins and affect the structures and dynamics of membraneless organelles (Lee *et al.*, 2016; Lin *et al.*, 2016), they could also directly affect the P-body formation while promoting stress granule formation in parallel. Unlike stress granules, P-bodies are much less dynamic structures, as determined by FRAP of fluorescence-tagged DCP1α (unpublished data). Therefore, the consequences of the disruption of P-bodies could be long-lasting. Although P-body formation is not entirely required for NMD (Eulalio *et al.*, 2007), NMD activities would likely be affected by the displacement of various NMD-related proteins residing in P-bodies.

One key finding from study is that the NMD pathway would be a promising downstream checkpoint for therapeutic intervention in cellular and *in vivo* models of *C9orf72* ALS. This conclusion has provided strong evidence to support the emerging concept that NMD could be a therapeutic target for some ALS cases (Jaffrey and Wilkinson, 2018). Previous studies have shown beneficial effects of UPF1 in a TDP-43 rat model and FUS/TDP-43 cellular models (Barmada *et al.*, 2015; Jackson *et al.*, 2015), although the mechanisms were not clear. Our new findings strongly suggested that the NMD pathway could be a converging therapeutic target in ALS/FTD cases with a strong RNA dysregulation component, such as aberrant alternative splicing.

The beneficial effects of tranilast (*N*-[3,4-dimethoxycinnamoyl]-anthranilic acid; trade name: Rizaben) in our *C9orf72* HRE models are encouraging. Tranilast has been used in Japan, South Korea and China to treat bronchial asthma since 1982 (Rogosnitzky *et al.*, 2012; Darakhshan and Pour, 2015). It is a synthetic derivative of the tryptophan metabolite anthranilic acid, and has been shown to suppress autoimmunity in a mouse model of multiple sclerosis (Platten *et al.*, 2005) and tested for the treatment of various proliferative disorders (Rogosnitzky *et al.*, 2012). The exact molecular mechanism of tranilast action is unclear, but its current clinical applications could be due to its ability to suppress immune response, inflammation, histamine release and the TGF-β pathway (Darakhshan and Pour, 2015). Whether these effects are related to the ability of tranilast to activate NMD remains to be investigated. Tranilast-mediated immune suppression could be a consequence of NMD activation. We found that immune response-related NMD target genes are significantly enriched in the *C9orf72* ALS brains, in which the NMD pathway is inhibited (Supplementary Table 2), thus further suggesting the potential beneficial effect of tranilast in *C9orf72* ALS patients.

Overall, the long track record of tranilast as a well-tolerated, low toxicity drug would make it a highly promising choice for ALS therapy. A daily dose of 600 mg has been used in patients for tumour treatment, and orally-administered tranilast could pass the blood–brain barrier (Darakhshan and Pour, 2015). Therefore, it will be important to fully characterize the therapeutic effects of tranilast in other *C9orf72* animal models, as well as in other ALS models. Tranilast clinical trials in ALS patients, particularly those carrying the *C9orf72* HRE, could be attempted to meet the urgent need for new ALS therapies. With validation of its protective effect against *C9orf72* HRE, tranilast may also be used in individuals carrying *C9orf72* HRE at

pre-symptomatic stage to delay or prevent the disease onset.

Acknowledgements

We thank Bloomington *Drosophila* Stock Center and core facility of *Drosophila* resource and technology at Shanghai Institutes for Biological Sciences for various fly lines. We thank Dr Adrian Isaacs for providing the original *C9orf72* DPRs *Drosophila* lines, related plasmids and key discussion. We also thank Dr Yusama Ishida for the UPF1 plasmid and Dr Fude Huang for various fly strains. We thank Libing Shen from the Bioinformatics Core Facility at ION for his help in RNA-Seq data analysis, and Jialing Li and Qiuhong Li for technical assistance.

Funding

This work was supported by National Science Foundation of China grant (81771425); Hundreds of Talents Program to J.X., Chinese Academy of Sciences; Shanghai Pujiang Talent Program (12PJ1410000) to J.X.; Natural Science Foundation of Shanghai Grant (16ZR1448800) to H.-F.W. National Institute of Health (NIH RO1 NS085207) to R.S.; Muscular Dystrophy Association and ALS Association (16-IIP-278) to R.S.

Competing interests

J.X and W.C.X. are co-inventors of patent application (CN201710646727) 'The use of nonsense-mediated mRNA decay in the treatment and diagnosis of neurodegenerative diseases'.

Supplementary material

Supplementary material is available at *Brain* online.

References

Abe K, Aoki M, Tsuji S, Itoyama Y, Sobue G, Togo M, et al. Safety and efficacy of edaravone in well defined patients with amyotrophic lateral sclerosis: a randomised, double-blind, placebo-controlled trial. Lancet Neurol 2017; 16: 505–12.

Anders S, Huber W. Differential expression analysis for sequence count data. Genome Biol 2010; 11: R106.

Ash PE, Bieniek KF, Gendron TF, Caulfield T, Lin W-L, DeJesus-Hernandez M, et al. Unconventional translation of C9ORF72 GGGGCC expansion generates insoluble polypeptides specific to c9FTD/ALS. Neuron 2013; 77: 639–46.

Barmada SJ, Ju S, Arjun A, Batarse A, Archbold HC, Peisach D, et al. Amelioration of toxicity in neuronal models of amyotrophic lateral sclerosis by hUPF1. Proc Natl Acad Sci 2015; 112: 7821–6.

Bensimon G, Lacomblez L, Meininger V. A controlled trial of riluzole in amyotrophic lateral sclerosis. ALS/Riluzole Study Group. N Engl J Med 1994; 330: 585–91.

Bhuvanagiri M, Schlitter AM, Hentze MW, Kulozik AE. NMD: RNA biology meets human genetic medicine. Biochem J 2010; 430: 365–77.

Boelz S, Neu-Yilik G, Gehring NH, Hentze MW, Kulozik AE. A chemiluminescence-based reporter system to monitor nonsense-mediated mRNA decay. Biochem Biophys Res Commun 2006; 349: 186–91.

Boeynaems S, Bogaert E, Kovacs D, Konijnenberg A, Timmerman E, Volkov A, et al. Phase separation of C9orf72 dipeptide repeats perturbs stress granule dynamics. Molecular Cell 2017; 65: 1044–55.e5.

Bramham CR, Worley PF, Moore MJ, Guzowski JF. The immediate early gene Arc/Arg3.1: regulation, mechanisms, and function. J Neurosci 2008; 28: 11760–7.

Chapin A, Hu H, Rynearson SG, Hollien J, Yandell M, Metzstein MM. In vivo determination of direct targets of the nonsense-mediated decay pathway in drosophila. G3: Genes|Genomes|Genetics 2014; 4: 485–96.

Cheng W, Wang S, Mestre AA, Fu C, Makarem A, Xian F, et al. C9ORF72 GGGGCC repeat-associated non-AUG translation is upregulated by stress through eIF2α phosphorylation. Nature Commun 2018; 9: 51.

Connolly JB. Neurodegeneration caused by the translation of nonsense: does macromolecular misfolding impair the synchrony of gene expression? Med Hypotheses 2005; 64: 968–72.

Cooper-Knock J, Bury JJ, Heath PR, Wyles M, Higginbottom A, Gelsthorpe C, et al. C9ORF72 GGGGCC expanded repeats produce splicing dysregulation which correlates with disease severity in amyotrophic lateral sclerosis. PLoS One 2015; 10: e0127376.

Darakhshan S, Pour AB. Tranilast: A review of its therapeutic applications. Pharmacol Res 2015; 91: 15–28.

DeJesus-Hernandez M, Mackenzie Ian R, Boeve Bradley F, Boxer Adam L, Baker M, Rutherford Nicola J, et al. Expanded GGGGCC hexanucleotide repeat in noncoding region of C9ORF72 causes chromosome 9 p-Linked FTD and ALS. Neuron 2011; 72: 245–56.

Durand S, Cougot N, Mahuteau-Betzer F, Nguyen C-H, Grierson DS, Bertrand E, et al. Inhibition of nonsense-mediated mRNA decay (NMD) by a new chemical molecule reveals the dynamic of NMD factors in P-bodies. J Cell Biol 2007; 178: 1145–60.

Eulalio A, Behm-Ansmant I, Schweizer D, Izaurralde E. P-Body formation is a consequence, not the cause, of RNA-mediated gene silencing. Mol Cell Biol 2007; 27: 3970–81.

Fornace AJ, Jackman J, Hollander MC, Hoffman-Liebermann B, Liebermann DA. Genotoxic-stress-response genes and growth-arrest genes. Ann New York Acad Sci 1992; 663: 139–53.

Gendron TF, Petrucelli L. Disease mechanisms of C9ORF72 repeat expansions. Cold Spring Harb Perspect Med 2018; 8.

Gijselinck I, Cruts M, Van Broeckhoven C. The genetics of C9orf72 expansions. Cold Spring Harb Perspect Med 2018; 8. pii: a026757. doi: 10.1101/cshperspect.a026757.

Giorgi C, Yeo GW, Stone ME, Katz DB, Burge C, Turrigiano G, et al. The EJC factor eIF4AIII modulates synaptic strength and neuronal protein expression. Cell 2007; 130: 179–91.

Green KM, Glineburg MR, Kearse MG, Flores BN, Linsalata AE, Fedak SJ, et al. RAN translation at C9orf72-associated repeat expansions is selectively enhanced by the integrated stress response. Nature Commun 2017; 8: 2005.

He F, Jacobson A. Nonsense-mediated mRNA decay: degradation of defective transcripts is only part of the story. Annu Rev Genet 2015; 49: 339–66.

Hubstenberger A, Courel M, Benard M, Souquere S, Ernoult-Lange M, Chouaib R, et al. P-body purification reveals the condensation of repressed mRNA regulons. Mol Cell 2017; 68: 144–57.e5.

Jackson KL, Dayton RD, Orchard EA, Ju S, Ringe D, Petsko GA, et al. Preservation of forelimb function by UPF1 gene therapy in a

rat model of TDP-43-induced motor paralysis. Gene Ther 2015; 22: 20–8.
Jaffrey SR, Wilkinson MF. Nonsense-mediated RNA decay in the brain: emerging modulator of neural development and disease. Nat Rev Neurosci 2018; 19: 715–28.
Jiang X, Zhang T, Wang H, Wang T, Qin M, Bao P, et al. Neurodegeneration-associated FUS is a novel regulator of circadian gene expression. Transl Neurodegener 2018; 7: 24.
Kanekura K, Yagi T, Cammack AJ, Mahadevan J, Kuroda M, Harms MB, et al. Poly-dipeptides encoded by the C9ORF72 repeats block global protein translation. Hum Mol Genet 2016; 25: 1803–13.
Kedersha N, Stoecklin G, Ayodele M, Yacono P, Lykke-Andersen J, Fritzler MJ, et al. Stress granules and processing bodies are dynamically linked sites of mRNP remodeling. J Cell Biol 2005; 169: 871–84.
Keeling KM, Wang D, Dai Y, Murugesan S, Chenna B, Clark J, et al. Attenuation of nonsense-mediated mRNA decay enhances in vivo nonsense suppression. PLoS ONE 2013; 8: e60478.
Kervestin S, Jacobson A. NMD: a multifaceted response to premature translational termination. Nat Rev Mol Cell Biol 2012; 13: 700–12.
Kwon I, Xiang S, Kato M, Wu L, Theodoropoulos P, Wang T, et al. Poly-dipeptides encoded by the C9orf72 repeats bind nucleoli, impede RNA biogenesis, and kill cells. Science 2014; 345: 1139–45.
Lee KH, Zhang P, Kim HJ, Mitrea DM, Sarkar M, Freibaum BD, et al. C9orf72 Dipeptide Repeats impair the assembly, dynamics, and function of membrane-less organelles. Cell 2016; 167: 774–88.e17.
Lee YB, Baskaran P, Gomez J, Chen HJ, Nishimura A, Smith B, et al. C9orf72 poly GA RAN-translated protein plays a key role in Amyotrophic Lateral Sclerosis via aggregation and toxicity. Hum Mol Genet 2017; 26: 4765–77.
Lewis BP, Green RE, Brenner SE. Evidence for the widespread coupling of alternative splicing and nonsense-mediated mRNA decay in humans. Proc Natl Acad Sci 2003; 100: 189–92.
Li Z, Vuong JK, Zhang M, Stork C, Zheng S. Inhibition of nonsense-mediated RNA decay by ER stress. RNA 2017; 23: 378–94.
Lin Y, Mori E, Kato M, Xiang S, Wu L, Kwon I, et al. Toxic PR poly-dipeptides encoded by the C9orf72 repeat expansion target LC domain polymers. Cell 2016; 167: 789–802. e12.
Ling S-C, Polymenidou M, Cleveland Don W. Converging mechanisms in ALS and FTD: disrupted RNA and protein homeostasis. Neuron 2013; 79: 416–38.
Liu H, Han M, Li Q, Zhang X, Wang W-A, Huang F-D. Automated rapid iterative negative geotaxis assay and its use in a genetic screen for modifiers of Aβ42-induced locomotor decline in Drosophila. Neurosci Bull 2015; 31: 541–9.
Lykke-Andersen S, Jensen TH. Nonsense-mediated mRNA decay: an intricate machinery that shapes transcriptomes. Nat Rev Mol Cell Biol 2015; 16: 665–77.
Mackenzie IR, Nicholson AM, Sarkar M, Messing J, Purice MD, Pottier C, et al. TIA1 mutations in amyotrophic lateral sclerosis and frontotemporal dementia promote phase separation and alter stress granule dynamics. Neuron 2017; 95: 808–16.e9.
May S, Hornburg D, Schludi M, Arzberger T, Rentzsch K, Schwenk B, et al. C9orf72 FTLD/ALS-associated Gly-Ala dipeptide repeat proteins cause neuronal toxicity and Unc119 sequestration. Acta Neuropathol 2014; 128: 485–503.
Mendell JT, Sharifi NA, Meyers JL, Martinez-Murillo F, Dietz HC. Nonsense surveillance regulates expression of diverse classes of mammalian transcripts and mutes genomic noise. Nat Genet 2004; 36: 1073–8.
Mizielinska S, Gronke S, Niccoli T, Ridler CE, Clayton EL, Devoy A, et al. C9orf72 repeat expansions cause neurodegeneration in Drosophila through arginine-rich proteins. Science 2014; 345: 1192–4.
Mori K, Weng S-M, Arzberger T, May S, Rentzsch K, Kremmer E, et al. The C9orf72 GGGGCC repeat is translated into aggregating dipeptide-repeat proteins in FTLD/ALS. Science 2013; 339: 1335–8.
Nelson JO, Moore KA, Chapin A, Hollien J, Metzstein MM. Degradation of Gadd45 mRNA by nonsense-mediated decay is essential for viability. eLife 2016; 5: e12876.
Nguyen AD, Nguyen TA, Zhang JS, Devireddy S, Zhou P, Karydas AM, et al. Murine knockin model for progranulin-deficient frontotemporal dementia with nonsense-mediated mRNA decay. Proc Natl Acad Sci USA 2018; 115: E2849–E58.
Nguyen LS, Jolly L, Shoubridge C, Chan WK, Huang L, Laumonnier F, et al. Transcriptome profiling of UPF3B/NMD-deficient lymphoblastoid cells from patients with various forms of intellectual disability. Mol Psychiatry 2012; 17: 1103–15.
Nickless A, Jackson E, Marasa J, Nugent P, Mercer RW, Piwnica-Worms D, et al. Intracellular calcium regulates nonsense-mediated mRNA decay. Nat Med 2014; 20: 961–6.
Parker R, Sheth U. P bodies and the control of mRNA translation and degradation. Molecular Cell 2007; 25: 635–46.
Platten M, Ho PP, Youssef S, Fontoura P, Garren H, Hur EM, et al. Treatment of autoimmune neuroinflammation with a synthetic tryptophan metabolite. Science 2005; 310: 850–5.
Popp MW, Maquat LE. Nonsense-mediated mRNA decay and cancer. Curr Opin Genet Dev 2018; 48: 44–50.
Protter DSW, Parker R. Principles and properties of stress granules. Trends Cell Biol 2016; 26: 668–79.
Prudencio M, Belzil VV, Batra R, Ross CA, Gendron TF, Pregent LJ, et al. Distinct brain transcriptome profiles in C9orf72-associated and sporadic ALS. Nat Neurosci 2015; 18: 1175–82.
Renton AE, Chio A, Traynor BJ. State of play in amyotrophic lateral sclerosis genetics. Nat Neurosci 2014; 17: 17–23.
Renton Alan E, Majounie E, Waite A, Simón-Sánchez J, Rollinson S, Gibbs JR, et al. A hexanucleotide repeat expansion in C9ORF72 is the cause of chromosome 9p21-linked ALS-FTD. Neuron 2011; 72: 257–68.
Rogosnitzky M, Danks R, Kardash E. Therapeutic potential of tranilast, an anti-allergy drug, in proliferative disorders. Anticancer Res 2012; 32: 2471–8.
Schludi M, May S, Grässer F, Rentzsch K, Kremmer E, Küpper C, et al. Distribution of dipeptide repeat proteins in cellular models and C9orf72 mutation cases suggests link to transcriptional silencing. Acta Neuropathol 2015: 130: 537–55.
Schludi MH, Becker L, Garrett L, Gendron TF, Zhou Q, Schreiber F, et al. Spinal poly-GA inclusions in a C9orf72 mouse model trigger motor deficits and inflammation without neuron loss. Acta Neuropathol 2017: 134: 241–54.
Sheth U, Parker R. Targeting of aberrant mRNAs to cytoplasmic processing bodies. Cell 2006; 125: 1095–109.
Shi Y, Lin S, Staats KA, Li Y, Chang WH, Hung ST, et al. Haploinsufficiency leads to neurodegeneration in C9ORF72 ALS/FTD human induced motor neurons. Nat Med 2018; 24: 313–25.
Shukla S, Parker R. Hypo- and hyper-assembly diseases of RNA–protein complexes. Trends Mol Med 2016; 22: 615–28.
Skoglund L, Brundin R, Olofsson T, Kalimo H, Ingvast S, Blom ES, et al. Frontotemporal dementia in a large Swedish family is caused by a progranulin null mutation. Neurogenet 2009; 10: 27–34.
Son HG, Seo M, Ham S, Hwang W, Lee D, An SWA, et al. RNA surveillance via nonsense-mediated mRNA decay is crucial for longevity in daf-2/insulin/IGF-1 mutant C. elegans. Nat Commun 2017; 8: 14749.
Tabrez SS, Sharma RD, Jain V, Siddiqui AA, Mukhopadhyay A. Differential alternative splicing coupled to nonsense-mediated decay of mRNA ensures dietary restriction-induced longevity. Nat Commun 2017; 8: 306.
Tao Z, Wang H, Xia Q, Li K, Jiang X, Xu G, et al. Nucleolar stress and impaired stress granule formation contribute to C9orf72 RAN translation-induced cytotoxicity. Hum Mol Genet 2015; 24: 2426–41.

Taylor JP, Brown RH Jr, Cleveland DW. Decoding ALS: from genes to mechanism. Nat 2016; 539: 197–206.

Tran H, Almeida S, Moore J, Gendron Tania F, Chalasani U, Lu Y, et al. Differential toxicity of nuclear RNA foci versus dipeptide repeat proteins in a drosophila model of C9ORF72 FTD/ALS. Neuron 2015; 87: 1207–14.

Wittmann J, Hol EM, Jäck H-M. hUPF2 silencing identifies physiologic substrates of mammalian nonsense-mediated mRNA decay. Mol Cell Biol 2006; 26: 1272–87.

Xu W, Xu J. C9orf72 dipeptide repeats cause selective neurodegeneration and cell-autonomous excitotoxicity in Drosophila glutamatergic neurons. J Neurosci 2018; 38: 7741–52.

Youn JY, Dunham WH, Hong SJ, Knight JDR, Bashkurov M, Chen GI, et al. High-density proximity mapping reveals the subcellular organization of mRNA-associated granules and bodies. Mol Cell 2018; 69: 517–32.e11.

Zhang K, Daigle JG, Cunningham KM, Coyne AN, Ruan K, Grima JC, et al. Stress granule assembly disrupts nucleocytoplasmic transport. Cell 2018a; 173: 958–71.e17.

Zhang Y-J, Jansen-West K, Xu Y-F, Gendron TF, Bieniek KF, Lin W-L, et al. Aggregation-prone c9FTD/ALS poly(GA) RAN-translated proteins cause neurotoxicity by inducing ER stress. Acta Neuropathol 2014; 128: 505–24.

Zhang YJ, Gendron TF, Ebbert MTW, O'Raw AD, Yue M, Jansen-West K, et al. Poly(GR) impairs protein translation and stress granule dynamics in C9orf72-associated frontotemporal dementia and amyotrophic lateral sclerosis. Nat Med 2018b; 24: 1136–42.

Zhang YJ, Gendron TF, Grima JC, Sasaguri H, Jansen-West K, Xu YF, et al. C9ORF72 poly(GA) aggregates sequester and impair HR23 and nucleocytoplasmic transport proteins. Nat Neurosci 2016; 19: 668–77.